When treated in a probabilistic manner, it is demonstrated that these equations can be utilized to predict the standard deviations in crosstrack and downtrack errors. Such prediction capability allows these equations to be used as an AQI. This algorithm permits one to decide when to terminate the transfer alignment process of a guided weapon by predicting, at selected times in the alignment process, the crosstrack and/or downtrack error uncertainties that would result after flyout to the area where the first navigational update is expected. Usage of a covariance simulation has shown that the AQI predicted crosstrack error uncertainty at the end of transfer alignment agrees satisfactorily with the actual crosstrack error uncertainty at the end of unaided flyout, as deduced from the system covariance matrix.

References

[1]Pitman, G. R., Jr. (ed.), *Inertial Guidance*, Wiley, New York, 1962, pp. 166–169.

[2]Broxmeyer, C., *Inertial Navigation Systems*, McGraw–Hill, New York, 1964, pp. 144–147.

[3]Britting, K. R., *Inertial Navigation Systems Analysis*, Wiley-Interscience, New York, 1971, pp. 126–152.

[4]Levinson, E., "Laser-Gyro Strapdown Inertial System Applications," AGARD Lecture Series, No. 95, 1978, pp. 6–47, 6–48.

[5]Bar-Itzhack, I. Y., and Berman, N., "Control Theoretic Approach to Inertial Navigation Systems," *Journal of Guidance, Control, and Dynamics*, Vol. 11, No. 3, 1988, pp. 237–245.

[6]Kreyszig, E., *Advanced Engineering Mathematics*, 8th ed., Wiley, New York, 1999, Chap. 3.

[7]Bose, S. C., *Integrated Navigation Systems (GPS/INS)*, Lecture Notes, Technalytics Inc., OH, 1996, Chap. 27.

Payload Mass Fractions for Minimum-Time Trajectories of Flat and Compound Solar Sails

Colin R. McInnes*
University of Glasgow, Glasgow, Scotland G12 8QQ, United Kingdom

I. Introduction

ALMOST all solar sail mission studies documented in the published literature have considered conventional flat solar sail configurations. There is, however, an alternative configuration, which appears to offer greater performance than the flat solar sail. Compound solar sails separate the functions of collecting and directing solar radiation by using a large sun-facing collector. This collector then directs light onto a small secondary directing mirror, attached to the collector by a boom. While the main collector is fixed in a sun-facing attitude, the director is rotated to control the direction of the thrust exerted by the compound sail.

It can be shown that the thrust exerted by an ideal flat solar sail is proportional to $\cos^2 u$, where u is the angle between the sun line and the sail thrust vector, the so-called cone angle. However, for an ideal compound solar sail, it can be shown that the thrust is proportional to $\cos u$ (Ref. 1). As such, the compound sail appears more efficient than conventional flat solar sails for orbit transfer. The compound solar sail concept was originally proposed in the Soviet literature[2] in the early 1970s and was subsequently reinvented by Forward.[3] Although the concept appears attractive in principle, as yet no detailed engineering design studies have been undertaken for this solar sail configuration. In particular, the effect of losses along the optical path has yet to be addressed.

In this Note, a minimum-time steering law will be derived for a compound solar sail, which complements existing steering laws for flat solar sails. The potential benefits of compound solar sails will be investigated by calculating the increase in payload mass delivered by a compound solar sail for a simple Earth–Mars transfer problem.

II. Minimum-Time Trajectories

To assess the performance of the compound solar sail, a steering law for minimum-time trajectories will be determined using the Pontryagin principle. Many authors have investigated minimum-time trajectories for flat solar sails, although here the succinct analysis of Ref. 4 is followed. The equations of motion for a solar sail in heliocentric orbit will be defined using nondimensional units as

$$\dot{x}_1 = x_2 \tag{1a}$$

$$\dot{x}_2 = x_3^2/x_1 - 1/x_1^2 + \beta\left(1/x_1^2\right)\cos^m u \cos u, \qquad m = 1, 2 \tag{1b}$$

$$\dot{x}_3 = -(x_2 x_3/x_1) + \beta\left(1/x_1^2\right)\cos^m u \sin u, \qquad m = 1, 2 \tag{1c}$$

$$\dot{x}_4 = x_3/x_1 \tag{1d}$$

where x_1 is the solar sail orbit radius, x_2 is the radial velocity, x_3 is the circumferential velocity, and x_4 is the polar angle of the solar sail from some reference direction. Here, the orbit radius is nondimensional with respect to the initial orbit radius whereas the velocities are nondimensional with respect to the initial circular orbit speed. With these nondimensional units, β becomes the ratio of the solar radiation pressure acceleration to the solar gravitational acceleration experienced by the solar sail. This parameter is often termed the sail lightness number.[1] The index m is used to define the type of solar sail, with $m = 2$ corresponding to a flat solar sail and $m = 1$ corresponding to a compound solar sail.

The optimal control problem is now to minimize the trip time and, hence, the following performance index:

$$J = t_f \tag{2}$$

When the Pontryagin principle is used, the Hamiltonian of the problem can be defined using costates (λ_1, λ_2, and λ_3) for each of the three states (x_1, x_2, and x_3). When these costates are used, it can be shown that

$$H = \lambda_1 x_2 + \lambda_2\left[x_3^2/x_1 - 1/x_1^2 + \beta\left(1/x_1^2\right)\cos^m u \cos u\right] + \lambda_3\left[-x_2 x_3/x_1 + \beta\left(1/x_1^2\right)\cos^m u \sin u\right] \tag{3}$$

The optimal control is now found by minimizing the Hamiltonian with respect to the control variable u. From Eq. (3), it is found that

$$\frac{\partial H}{\partial u} = \beta\frac{1}{x_1^2}\left[-\lambda_2(m+1)\cos^m u \sin u + \lambda_3(\cos^{m+1} u - m\cos^{m-1} u \sin^2 u)\right] \tag{4}$$

Therefore, it can be seen that the Hamiltonian is now stationary with respect to the control variable u under the following conditions:

$$\cos u = 0 \tag{5a}$$

$$m\lambda_3 \tan^2 u + \lambda_2(m+1)\tan u - \lambda_3 = 0 \tag{5b}$$

Furthermore, using Eq. (5b), it can be shown that the Hamiltonian is minimized for a flat solar sail and compound solar sail using the following controls for the optimum solar sail cone angle $\bar{u}$; namely,

$$\tan\bar{u} = \left(-3\lambda_2 - \sqrt{9\lambda_2^2 + 8\lambda_3^2}\right)\Big/ 4\lambda_3, \qquad m = 2 \tag{6a}$$

$$\tan\bar{u} = \left(-\lambda_2 - \sqrt{\lambda_2^2 + \lambda_3^2}\right)\Big/ \lambda_3, \qquad m = 1 \tag{6b}$$

It is found that Eq. (6a) is identical to the steering law derived in other studies of minimum-time trajectories for flat solar sails, as

Received 17 September 1999; revision received 3 July 2000; accepted for publication 19 July 2000.

*Professor, Department of Aerospace Engineering; colinmc@aero.gla.ac.uk.

expected. However, Eq. (6b) provides a new steering law for the compound solar sail.

To obtain the control time history, it is necessary to obtain the costates as a function of time. The costate equations are now derived from the Hamiltonian using $\dot{\lambda}_i = -\partial H/\partial x_i (i = 1-3)$ in the usual manner to obtain

$$\dot{\lambda}_1 = -\lambda_2\left[-x_3^2/x_1^2 + 2/x_1^3 - 2\beta\left(1/x_1^3\right)cos^m u \cos u\right] - \lambda_3\left[x_2 x_3/x_1^2 - 2\beta\left(1/x_1^3\right)\cos^m u \sin u\right] \tag{7a}$$

$$\dot{\lambda}_2 = -\lambda_1 + \lambda_3(x_3/x_1) \tag{7b}$$

$$\dot{\lambda}_3 = -2\lambda_2(x_3/x_1) + \lambda_3(x_2/x_1) \tag{7c}$$

In addition, a transversality condition must be satisfied because the final time is to be optimized:

$$H(t_f) + 1 = 0 \tag{8}$$

To assess the relative performance of a flat and compound solar sail, minimum-time trajectories from Earth to Mars will be considered. For ease of illustration, it will be assumed that the transfer is between circular, coplanar orbits from $x_1(0) = 1$, $x_2(0) = 0$, and $x_3(0) = 1$ to $x_1(t_f) = 1.525$, $x_2(t_f) = 0$, and $x_3(t_f) = 0.8098$. The boundary conditions to be satisfied represent one of the standard benchmark problems used for low-thrust trajectory optimization.

The state and costate equations can now be integrated using the appropriate optimal control for the solar sail cone angle. To satisfy the boundary conditions and the transversality condition of the problem, Newton's method was used to obtain the initial costates. The trip times obtained for the flat solar sail using Eq. (6a), shown in Fig. 1, agree with other published data. Here, dimensional units have been inserted, where the solar sail characteristic acceleration is defined as the acceleration experienced when the cone angle $u = 0$ and the solar sail is at a heliocentric distance of 1 astronomical unit (AU). The corresponding trip times for the compound solar sail using Eq. (6b) are also shown in Fig. 1. It can be seen that the compound solar sail offers a reduction in trip time over a flat solar sail. More important, for a fixed trip time, the required compound solar sail characteristic acceleration can be significantly less than that required for a flat solar sail.

III. Payload Mass Fraction

Whereas the reduction in trip time offered by the compound solar sail appears attractive, the most useful benefit is the reduction in required characteristic acceleration for a fixed trip time. If the mass penalty for the additional complexity of the compound solar sail is not too great, significant increases in payload mass fraction appear possible. Such increases in payload mass fraction can result in a lower launch mass and, hence, lower mission costs. For illustration, the simple Earth–Mars trajectory discussed in Sec. II will be considered.

Because the force exerted on an ideal flat solar sail is given by $2PA$, where P is the incident light pressure, and A is the sail area, the solar sail characteristic acceleration is defined as $a_c = 2P_0/\sigma$, where σ is the total mass per unit area, or loading, of the solar sail, and P_0 is the solar radiation pressure at 1 AU. When the sail assembly loading σ_s is defined as the mass per unit area of the sail film and its supporting structure, the characteristic acceleration may be written as

$$a_c = \frac{2P_0}{\sigma_s + m_p/A} \tag{9}$$

where m_p is the payload mass of the solar sail. If the total mass of the solar sail is m_T, the payload mass may be written in terms of the total mass as

$$m_p^f = \left(1 - \sigma_s a_c^f/2P_0\right)m_T \tag{10}$$

where the superscript f refers to a flat solar sail and $m_T = m_p + \sigma_s A$. For the compound solar sail, it will be assumed that the sail reflector

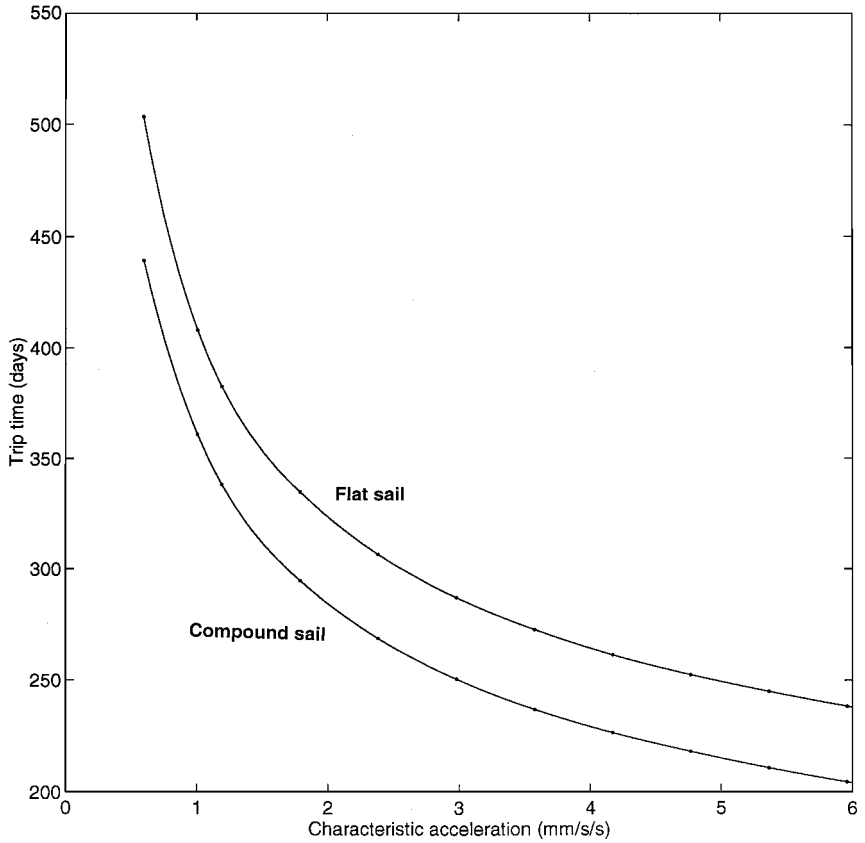

Fig. 1 Trip time as a function of characteristic acceleration.

Table 1 Payload mass delivered for a range of trip times

Trip time (days)	350	300	250
a_c^f, mm s^{-2}	1.60	2.59	4.97
a_c^c, mm s^{-2}	1.10	1.72	3.01
σ_s, g m^{-2}	3.5	2.5	1.5
m_T, kg	375	375	375
m_p^f, kg	144.7	108.9	68.5
m_p^c, kg			
$\kappa = 0.1$	200.9	180.9	170.8
$\kappa = 0.2$	185.0	163.2	152.2
Δm_p, kg			
$\kappa = 0.1$	56.1	71.0	102.3
$\kappa = 0.2$	40.3	54.3	83.8
κ^*	0.45	0.51	0.65

has the same properties as the flat sail. However, a penalty will be added to account for the additional mass required for the director mirror. Therefore, the assembly loading of the compound solar sail will be defined as $\sigma_s(1 + \kappa)$, for some mass penalty κ. The payload mass of the compound solar sail may then be written in terms of the total mass as

$$m_p^c = \left[1 - (1 + \kappa)\left(\sigma_s a_c^c \big/ 2P_0\right)\right] m_T \tag{11}$$

where the superscript c refers to a compound solar sail.

For a given trip time, the compound solar sail will in general be able to deliver a larger payload mass fraction than a flat solar sail. However, as the mass penalty for the compound solar sail increases the difference in payload mass fraction will of course fall. The break-even mass penalty κ^*, where both solar sails deliver the same payload mass, can be obtained by equating the payload masses defined by Eq. (10) and (11) to obtain

$$\kappa^* = a_c^f \big/ a_c^c - 1 \tag{12}$$

To provide an evaluation of the flat and compound solar sail, the payload mass delivered to Mars will be determined for a fixed launch mass of 375 kg, corresponding to the approximate $C_3 = 0$ capacity of the Taurus XL launch vehicle.

The delivered payload mass and increase in payload mass Δm_p have been determined for a range of trip times, as shown in Table 1. For the compound solar sail, a fixed mass penalty of 0.1 and 0.2 has been assumed. It can be seen that the benefit of the compound solar sail for long trip times of order 350 days is quite modest, corresponding to a 30% increase in delivered payload for a compound solar sail mass penalty of 0.2. However, for fast trip times of order 250 days, the benefit of the compound solar sail is more significant. Again, for a mass penalty of 0.2, the payload delivered by the compound solar sail is more than doubled. In this case the compound solar sail delivers a greater payload mass for a mass penalty of up to 0.65.

IV. Conclusions

A simple coplanar transfer problem has been used to derive a minimum-time steering law for a compound solar sail. It has been shown that, in principle, a compound solar sail can deliver a significantly greater payload mass fraction than a flat solar sail for short-trip times. Because the compound solar sail has not undergone the same level of detailed design that flat solar sails have, it remains to be seen whether mass penalties as low as 0.2 could be achieved in practice. If such configurations are possible, compound solar sails offer significant benefits for future fast missions.

References

[1]McInnes, C. R., *Solar Sailing: Technology, Dynamics and Mission Applications*, Springer–Praxis Series in Space Science and Technology, Springer-Verlag, Berlin, 1999, pp. 32–55.

[2]Malanin, V. V., and Repyakh, A. V., "On the Motion of a Craft with Two Solar Sails," *Problemy Mekhaniki Upravlyayemogo Dvizheniya*, No. 5, 1974, pp. 99–108.

[3]Forward, R. L., "Solar Photon Thrustor," *Journal of Spacecraft and Rockets*, Vol. 27, No. 4, 1990, pp. 411–416.

[4]Wood, L. J., Bauer, T. P., and Zondervan, K. P., "Comment on 'Time-Optimal Orbit Transfer Trajectory for Solar Sail Spacecraft,'" *Journal of Guidance and Control*, Vol. 5, No. 2, 1982, pp. 221–224.

Collision Dynamics for Space Tethers

Chris Blanksby* and Pavel Trivailo†
Royal Melbourne Institute of Technology, Melbourne, Victoria 3001, Australia

Introduction

OPERATION of tethers from large space structures such as the Space Shuttle Orbiter and, in the near future, the International Space Station (ISS) raises the possibility of collisions between the tether and parts of the structure. Such collisions could occur as a result of unstable retrieval, severance of the tether (and subsequent recoil), impact with space debris, or various other unscheduled events. The behavior of the system during such an event has not been considered in the literature, to the best of the authors' knowledge. An understanding of the dynamics of such an event is considered important in the development of contingency measures for minimizing risk.

This Note presents a methodology developed to examine the collision event. Numerical simulation results showing the details of a potential collision event involving the ISS are also presented.

For the purposes of this study, a lumped-mass model of the system is employed. As has been recognized in a number of papers,[1–4] the lumped-mass model is better able to deal with high curvature of the tether. This functionality is necessary to model the collision event, which would typically occur after the advent of extreme tether motion.

Theory

Tether Dynamics

The tether dynamics model uses a series of $n + 1$ lumped masses, connected together by n segments with linear stiffness, to represent the tether and is similar to that developed by Banerjee[4] or Banerjee and Do.[3] Some differences to these models exist in the application of Kane's equations to the system and in the means employed for deploying and retrieving the tether. The formulation of the equations of motion is such that they can be classified as Order-N, i.e., the computational effort required to solve for the acceleration vector of each body varies linearly with the number of bodies. Previous validations have shown the accuracy of the model to be within 5% for a range of situations.[5]

Environmental and system contributions to generalized forces included in the model are 1) gravitational force, 2) tether tension force, 3) electromagnetic force, 4) internal damping force, 5) aerodynamic force, and 6) arbitrary, applied force.

Collision

The model just described above has been enhanced to enable collisions to be modeled. In the present implementation only collisions between the tether and the space structure are considered; collisions between different segments of the tether are ignored. For the purposes of identifying locations of collisions, the space structure

Received 13 September 1999; revision received 22 May 2000; accepted for publication 26 July 2000.

*Doctoral Student, Department of Aerospace Engineering, GPO Box 2476V.

†Associate Professor, Department of Aerospace Engineering, GPO Box 2476V.